Assessment of Porites microatolls for paleothermometry: calibration for French Polynesia

Nicholas Farley, Antonioli Guillaume, Nadine Hallmann, Gilbert Camoin, Anton Eisenhauer, Claude Vella, Glenn A. Milne, Elias Samankassou

Assessment of *Porites* microatolls for paleothermometry: calibration for French Polynesia.

Farley Nicholas[1], Antonioli Guillaume[1], Hallmann Nadine[2], Camoin Gilbert[2], Eisenhauer Anton[3], Vella Claude[2], Milne Glenn A[4], Samankassou Elias[1]

[1]University of Geneva, Department of Earth Sciences, Rue des Maraîchers 13, CH-1205 Geneva, Switzerland

[2]Aix-Marseille Université, CNRS, IRD, INRAE, Collège de France, CEREGE, Europôle Méditerranéen de l'Arbois, BP80, 13545 Aix-en-Provence cedex 4, France

[3]GEOMAR Helmholtz-Zentrum für Ozeanforschung Kiel, Wischhofstraße 1-3, 24148 Kiel, Germany

[4]University of Ottawa, Department of Earth and Environmental Sciences, Ottawa, Ontario K1N 6N5, Canada

Abstract

Massive dome-shaped coral *Porites* are the predominant choice for paleoclimate studies due to their consistent and reliable growth. When growing close to sea level, they become limited in their vertical growth and form so-called 'microatolls'. Microatolls have not yet been extensively explored for paleoclimate reconstruction. Here, we investigate how reliable *Porites* microatolls are against empirical sea-surface temperature using Sr/Ca, δ18O, Li/Mg and Sr-U paleothermometry methods on modern *Porites* microatolls from the Society Islands, French Polynesia. Our results show Sr/Ca ratios have the lowest Standard Error of the Inverse Prediction (SEIP) at 0.415 °C (N = 41) with a calibration of Sr/Ca (mmol mol^{-1}) = -0.082 ± 0.006 SST (°C) + 11.256 ± 0.170 and with extremely good reproducibility across multiple corals. The reproducibility of $\delta^{18}O$ was not as good, with SEIP increasing to 0.829 °C (N = 41). Considering methods directly from the literature, Li/Mg ratio empirically corrected for Sr/Ca had the best balance between bias and precision where no local calibration was available. This study independently evaluates and confirms the suitability of *Porites* microatolls from well-flushed environments for paleoclimate studies. Fossil dome-shaped *Porites* grow anywhere between near-surface and roughly 20 m depths which inherently incorporates uncertainty into any sea surface temperature reconstruction. This uncertainty is significantly reduced for microatolls due to their well-constrained bathymetry. The study represents a fundamental step in paleoclimate research targeting consistently near the water-air interface bringing reliability. Combined with their ability to reconstruct past sea-level changes, microatolls have the potential to be central for future paleoenvironmental studies.

1. Introduction

The use of coral colonies as climate archives can extend the instrumental record, which reliably covers roughly 150 years (Parker et al., 2000). Unlike long-term deep-sea marine sediments, coral skeletons may record multiple centuries of past sea-surface conditions at a seasonal to monthly resolution under the right conditions. Coral records can therefore help to better understand the patterns and drivers of natural tropical climate variability, especially

the El Niño Southern Oscillation (ENSO) in the Pacific Ocean, which has global environmental consequences (Smith et al., 2016) and massive socio-economic impacts (Cashin et al., 2017).

Concentrations of geochemical tracers incorporated into the coral skeleton during its growth can provide valuable information on a range of environmental conditions. The Sr/Ca ratio is widely used to reconstruct sea-surface temperature (SST), with an inverse relationship first identified by Smith et al. (1979). The Mn/Ca ratios are a proxy for precipitation and runoff, as well as upwelling and wind speed (e.g. Inoue et al., 2014, Chen et al., 2015; Thompson et al., 2014; Yamano and Watanabe 2016). Other proxies, such as Li/Ca (Marriott et al., 2004), have shown a correlation with temperature. Stable oxygen isotopes ($\delta^{18}O$) have also been regularly used to reconstruct SST. Still, it has been demonstrated that this proxy can be influenced by sea-surface salinity (SSS). Therefore, it must be used in combination with other proxies, such as Sr/Ca (see review in Corrège, 2006). The reliability and reproducibility of the Sr/Ca ratio and $\delta^{18}O$ values have been questioned, as temperature reconstructions may vary considerably within the same reef or even within the same colony (Alibert & McCulloch, 1997; Alpert et al., 2017; Corrège, 2006; D'Olivo et al., 2018; de Villiers et al., 1994). These variations have been attributed to biological and physiochemical controls in the calcification process, referred-to as "vital effects", that are not yet fully understood (Gaetani & Cohen, 2006; Meibom et al., 2007). To overcome vital effects, Gaetani et al. (2011) proposed differential fractionation for different elements to extract the common temperature signal (for an overview see Sinclair, 2015). Two methods accounting for vital effects have recently been proposed: the Sr-U method (DeCarlo et al., 2016) and the Li/Mg universal thermometer (D'Olivo et al., 2018).

Porites colonies are one of the most sampled corals for paleoclimate reconstructions due to their clear growth pattern and their growth in a wide range of environments. In very shallow-water environments, their vertical growth may be constrained by exposure at lowest tides (Stoddart, 1969; McLean et al., 1978; Smithers and Woodroffe, 2001; Meltzner and Woodroffe, 2015; Hallmann et al., 2018) so that they continue to grow laterally to form so-called 'coral microatolls'. Their lateral growth rates range from 5 to 25 mm yr^{-1} (Woodroffe & McLean, 1990), comparable to those reported in dome-shaped *Porites* colonies. Coral microatolls have been used in sea-level reconstructions due to their strict environmental requirements (Hallmann et al., 2018, in press; Smithers & Woodroffe, 2001; Woodroffe & McLean, 1990; Yu et al., 2009). From a paleoenvironmental perspective, these requirements provide the unique advantage to obtain a record from a narrow depth range over extended periods. However, microatolls have barely been used to reconstruct climate variability, namely on Kiritimati (Christmas) Island (McGregor et al., 2011; Schoffield, 2011; Woodroffe et al., 2003) and the Great Barrier Reef (Roche et al., 2014).

This study aimed to assess the suitability and reliability of *Porites* microatolls for paleoclimate reconstructions. It relied on temperature reconstructions based on conventional geochemical analyses (element/Ca ratios and $\delta^{18}O$ values) and methods to correct for vital effects (Li/Mg and Sr-U) obtained on microatolls from the Society Islands, French Polynesia. The evaluation

of each method was then assessed based on the comparison between reconstructed temperatures and instrumental records with the primary goal to obtain a calibration that can be applied to fossil microatolls.

2. Methods

This study focused on microatolls from Bora Bora and Maupiti islands (French Polynesia, Central Southern Pacific), which are ~40 km apart on the Western end of Society Islands. Climate is tropical with two seasons, the austral summer from Nov-Apr being warm (28-29°C) and rainy, and the austral winter from May-Oct with cooler (23-25°C) temperatures and drier (Delesalle et al., 1985; Boiseau et al., 1998). Tides are semi-diurnal with a mean amplitude of 0.5m (Seard et al., 2011). The dominant wind patterns are the trade winds from the East/South-East to the North-East (Rashid et al., 2020). The samples BOB-47 and BOB-48 originated from the same microatoll in the northern part of Bora Bora (16°26'27.60"S, 151°45'42.42"W), and BOB-108 (16°32'39.84"S, 151°41'56.88"W) from a microatoll in the southeast (Green and orange respectively in Fig. 1). MAU-140 (16°25'7.98"S, 152°15'44.70"W) was sampled on Maupiti (blue in Fig. 1). All microatolls were collected at present day sea level in 2014 and 2015 on the protected reef facing the open ocean. All studied microatolls originated from well-flushed sites with direct contact to the open ocean. In this study, the Maupiti coral was studied in detail, and then the corals from Bora-Bora were used to assess the reproducibility and reliability of the original findings.

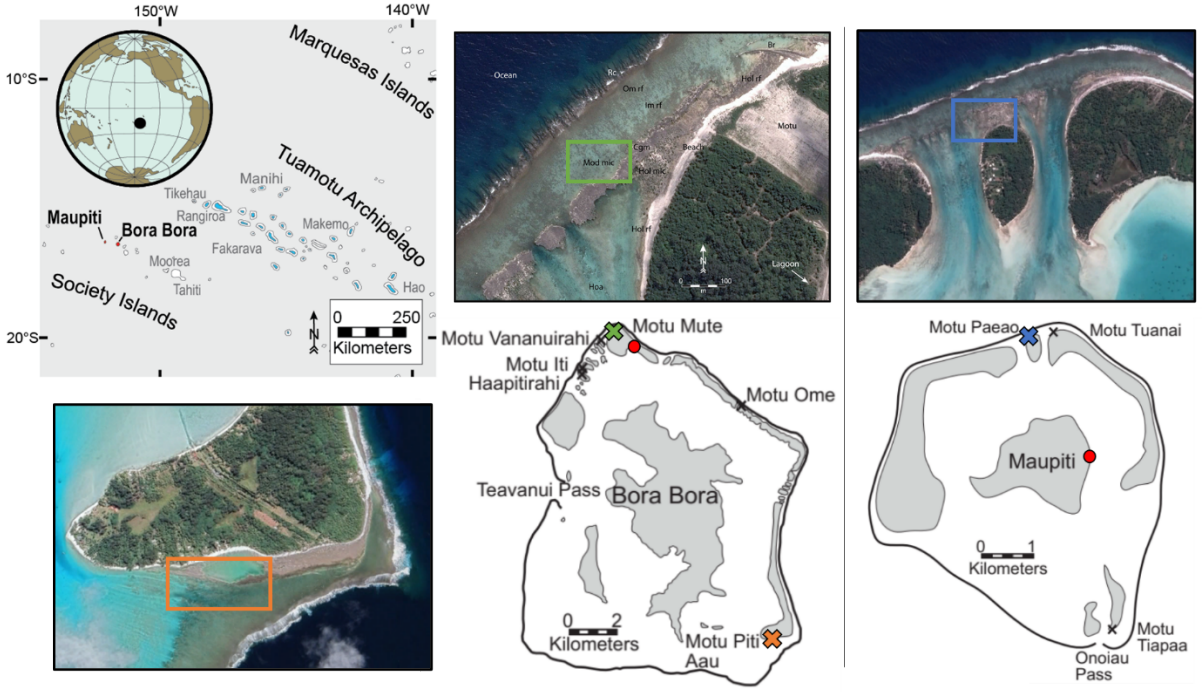

Figure 1 Location of sampled microatolls. On Bora-Bora sample BOB 47 and 48 from the North in Green and BOB-108 from the South in Orange. On Maupiti in the North coloured Blue. The red dots mark the position of Météo-France weather stations on the respective islands. Base

satellite images from Google Earth Pro, v 7.3.3.7699 Data SIO, NOAA, U.S. Navy, NGA. GEBCO. Images © 2020 CNES/Airbus.

In the laboratory, microatoll samples were sliced into 8 mm-thick slabs along the main growth axis and left 24 hours in diluted NaClO. The outer biological surface was removed and subsequently rinsed with distilled water (Grove et al., 2015). Small pieces of the slab were observed under a Scanning Electron Microscope (SEM) (Jeol JSM7001F) to screen for any early diagenetic alterations that could affect the geochemical signals in coral skeleton (Sayani et al., 2011; Felis et al., 2012; Krause et al., 2019). Sampling was carried out using a frame-mounted Dremel with a 1.0 mm drill bit, staggering each sample to ensure each drill hole is clearly isolated. Sampling protocol was following the central maximum growth axis (DeLong et al., 2013). The coral slabs were x-radiographed at the Quality Control SA (Lavaux, CH) imaging facility using a D7Pb film, with 100 kV exposures for 525 -750 mAs and a focal length of 1900 mm allowing to identify annual density bands and check exact sample positions along the growth axis.

The $\delta^{18}O$ and $\delta^{13}C$ values were measured on ThermoFinnigan Delta Plus XL (Gas Bench II) at the University of Lausanne, Switzerland, standardised against a Carrara marble standard and expressed relative to Vienna Pee Dee Belemnite (VPDB). The methods were adapted from Spoetl and Vennemann (2003). Average analytical error was ±0.1‰.

The concentrations of Ca, Sr, Mg and Ba were measured by Inductively Coupled Plasma Optical Emission Spectrometer (ICP-OES) (iCAP 3000 Duo, ThermoFisher Scientific) at the University of Geneva using a method adapted from Cantarero et al. (2017). An amount of 0.4 mg of coral powder was dissolved in 5% nitric acid to obtain a solution with Ca concentrations of roughly 40 ppm. Ba was measured on axial view allowing for greater sensitivity and lower detection limits. Internal yttrium standard was injected simultaneously to monitor machine stability, intermediate calibration (mixed from mono-element Agilent standards) samples were measured at regular intervals to monitor drift in each relevant element. External JCp-1 standards (Hathorne et al., 2013b; Okai et al., 2002) were measured at regular intervals throughout the run. For the sample MAU-140 (n = 15) run JCp-1 results were Sr/Ca 8.860 (SD = 0.036), Mg/Ca 4.176 (SD = 0.032) and Ba/Ca 7.733 (SD = 0.949). Across all samples measured on ICP-OES the standard errors changed slightly due to more variability in some runs: Sr/Ca (SD = 0.084), Mg/Ca (SD = 0.046) and Ba/Ca (SD = 0.927).

Trace elements of Li, B and U along with Ca, Sr, Mg, Ba were measured using ICP-MS (Agilent 7700x) at the University of Geneva. Samples were dissolved in 5% HNO_3 to obtain a solution including about 80 ppm Ca. Rhodium and Rhenium internal standards were run in parallel, and similar to the ICP-OES method above, intermediate calibration samples were included regularly through the run to monitor and correct drift in each relevant element along with JCp-1 standards (Hathorne et al., 2013a, b; Okai et al., 2002). The uncorrected JCp-1 values from the MAU-140 run were Sr/Ca 8.682 (SD 0.037), Mg/Ca 4.186 (SD 0.153) and Ba/Ca 6.956 (SD 0.336).

Météo-France land and ship-based instrumental temperatures were evaluated against high-resolution satellite data (see detail in supplementary material S1). The chosen dataset was the gridded 0.25° – 0.25° Advanced Very High Resolution Reconstructed Optimum Interpolation Sea Surface Temperature version 2 (AVHRR-OISSTv2) (Banzon et al., 2016; Reynolds et al., 2007). The temperature data was averaged to a monthly resolution (Antonioli, 2018).

The instrumental error was assessed (see details in supplementary material S2). Simple least squares linear regression of the proxy on temperature was used to evaluate the quality of fit and whether the relative abundance of other rare elements contributed significantly to the fitted model. The corresponding temperatures and 95% confidence intervals were estimated by inverse prediction from the fitted regression line (Draper & Smith, 1981, p 47; Neter et al., 1985). To make an inverse prediction, the estimated temperature and corresponding inverse confidence limits are read horizontally. The inverse confidence limits are known as the standard error of the inverse prediction (SEIP) (Demidenko et al., 2013). For more details and application of the equations, see supplementary material S3.

Slight variations in coral growth rates meant that the monthly averaged OISST and the sample mm scales did not match perfectly. For correspondence, peak matching and subsequent linear interpolation of the temperature values was carried out. The most recent datapoint was informed by the date of sample recovery with the outer edge surface of the coral skeleton, the living part during sample collection. The most recent turning point (maximum or minimum) in the analyte was matched to the most recent temperature turning point, while the oldest analyte turning point matched to the corresponding temperature turning point counting back in annual cycles. The tails either side of these two tie points were discarded from the calibration samples to reduce uncertainty and edge effects. As each tie point was added, the residual degrees of freedom in the linear regression analysis of the analyte on temperature was decreased by one. Doing so, the improvement in fit could be balanced with the loss of degrees of freedom to estimate residual error and avoid issues of overfitting. Results presented below for sample MAU-140 use the 'reduced peak to peak' dataset (n = 41), which is down from the total 54 datapoints and eliminated possible edge effects (for more information supplementary material S4).

3. Results and discussion

3.1. Preservation state and growth rate of the MAU-140 coral

X-radiography of the MAU-140 specimen showed very good alignment of the corallites with the slab cut relatively parallel (along) the dominant growth axis (Figure 2). The maximum growth axis was easily identifiable with the corallite growth and density bands. An average growth rate of 14.3 ± 0.5 mm year^{-1} was calculated based on measurements covering four years of continuous growth. The measured growth rate was consistent with previous data obtained on *Porites* microatolls (McGregor et al., 2011; Roche et al., 2014). SEM observations for MAU-140 reveal excellent preservation of the skeleton. No secondary aragonite or

diagenesis was identified near the outer edge or in the coral's internal structures and pores (for more detail and SEM images, see supplementary material S5).

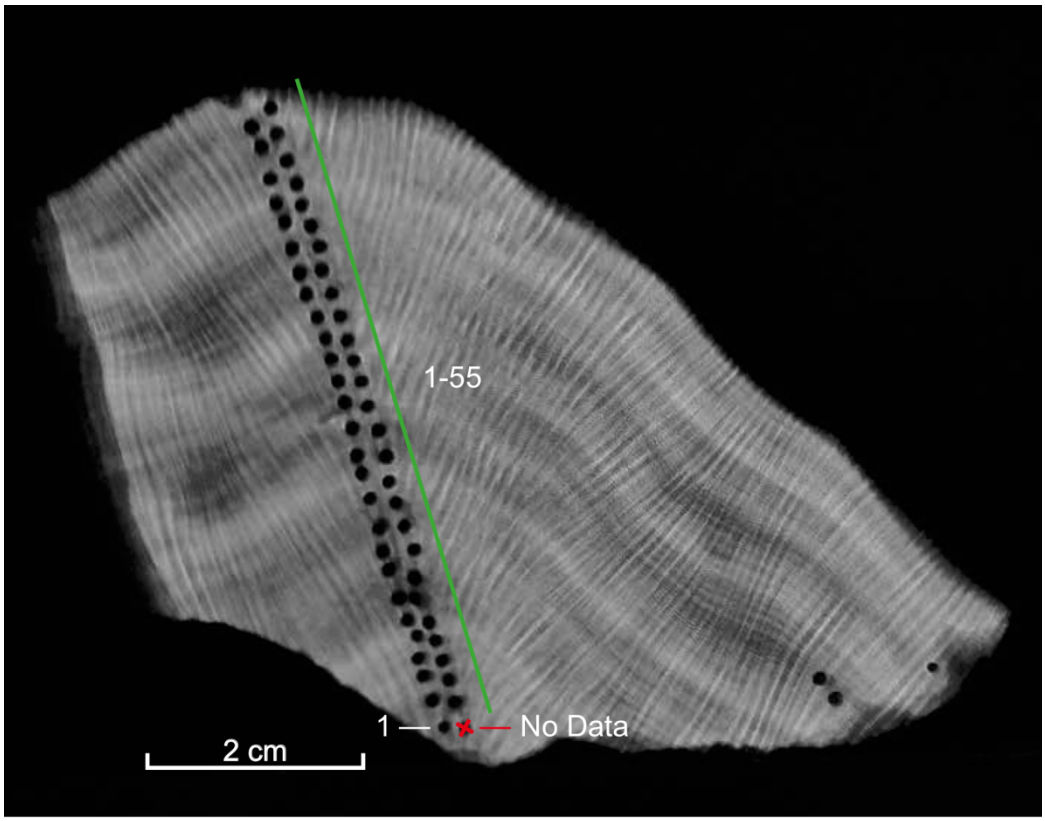

Figure 2 X-radiograph of MAU-140 with sampling path. The green line represents reliable sampling along the main growth axis and from the x-radiograph.

3.2. Comparison of calibrations from the literature on massive *Porites*

The calibration equations from various authors were applied directly to our data and compared using the mean and standard deviation of the difference between the fitted and actual SST (Table 1). In addition, the results from the 'universal' calibrations (i.e. applicable in any tropical region) and, where relevant, the local French Polynesian calibrations were included. The best fit for $\delta^{18}O$ was found with Cahyarini et al. (2008), but despite being a calibration from a nearby source, the Sr/Ca model was intermediate between the calibrations of Corrège (2006) and D'Olivo et al. (2018). As expected, the local calibration outperformed the universal calibrations, in this case only for $\delta^{18}O$ (Cahyarini et al., 2008) with a mean difference of 0.17 °C and a standard deviation of 0.64 °C. Note that for Sr/Ca the local calibration of Cahyarini et al. (2008) was not as accurate as the universal equation of D'Olivo et al. (2018) (larger mean difference); however, the local calibration produced a more precise result (lower standard deviation). The best universal calibration model was that of D'Olivo et al. (2018) using the Li/Mg method. While this method did not have the smallest mean or

standard deviation of the difference of all the methods assessed, it had the best balance between bias and precision as shown by the two metrics.

	Universal					Local	
	Li/Mg		Sr-U	Sr/Ca		Sr/Ca	$\delta^{18}O$
	D'Olivo et al. (2018) Empirical	Montagna et al. (2014)	DeCarlo et al. (2016)	Corrège (2006)	D'Olivo et al. (2018)	Cahyarini et al. (2008)	Cahyarini et al. (2008)
Mean °C	**1.967**	**1.908**	**-2.089**	**4.913**	**1.620**	**2.250**	**0.169**
SD °C	1.230	3.828	n.a.	0.817	4.059	0.902	0.636
Std err °C	0.194	0.605	n.a.	0.128	0.634	0.141	0.099

Table 1 Compilation of the mean difference between calibrations applied directly from the literature and the Optimal Interpolation Sea Surface Temperature (OISST) in °C.

3.3. Sr/Ca

For the analysed *Porites* microatoll sample, the fitted linear calibration for Sr/Ca was:

$$\textbf{Sr/Ca (mmol mol}^{-1}\textbf{) = -0.082 (±0.006) SST + 11.256 (±0.170)} \quad \textbf{(1)}$$

To estimate temperature from a new Sr/Ca ratio, the resulting inverted fitted regression equation was:

$$\textbf{SST = - (Sr/Ca - 11.256)/0.082} \quad \textbf{(2)}$$

with standard error of the inverse prediction (SEIP) 0.415 (±0.062) °C (See details on the calculation of SEIP in supplementary material S2).

The predicted temperatures from selected published models were compared in Figure 3. Although several studies using Sr/Ca were reported in the literature (see summary in Ross et al., 2019), comparison was limited to four references: the most widely referenced Sr/Ca calibration developed by Corrège (2006), the Sr/Ca calibration developed by D'Olivo et al. (2018) who proposed a universal method based on a combination of Sr/Ca and Li/Mg ratio, and the studies of Cahyarini et al. (2008) and Felis et al., (2012) using samples from Tahiti. It is worth noting these were all performed on massive *Porites* colonies in contrast to *Porites* microatolls of the present study. The results of the present study showed a steeper (more inverse slope) relationship to temperature with a greater intercept recorded in microatolls than in massive colonies (Figure 3).

The temperature reconstructions showed that the calibration curve of D'Olivo et al. (2018) displayed a good overlap for higher temperatures, but the shallower calibration slope meant the higher Sr/Ca values (inverse relationship) underestimated the temperatures (Figure 4).

Cahyarini et al. (2008) and Corrège (2006) reconstructed a very similar temperature range with a similar slope, but the absolute range was offset (different intercepts; Fig. 3). Our result is the most similar to the calibration from Felis et al., (2012), which was from massive *Porites* from the neighbouring island of Tahiti.

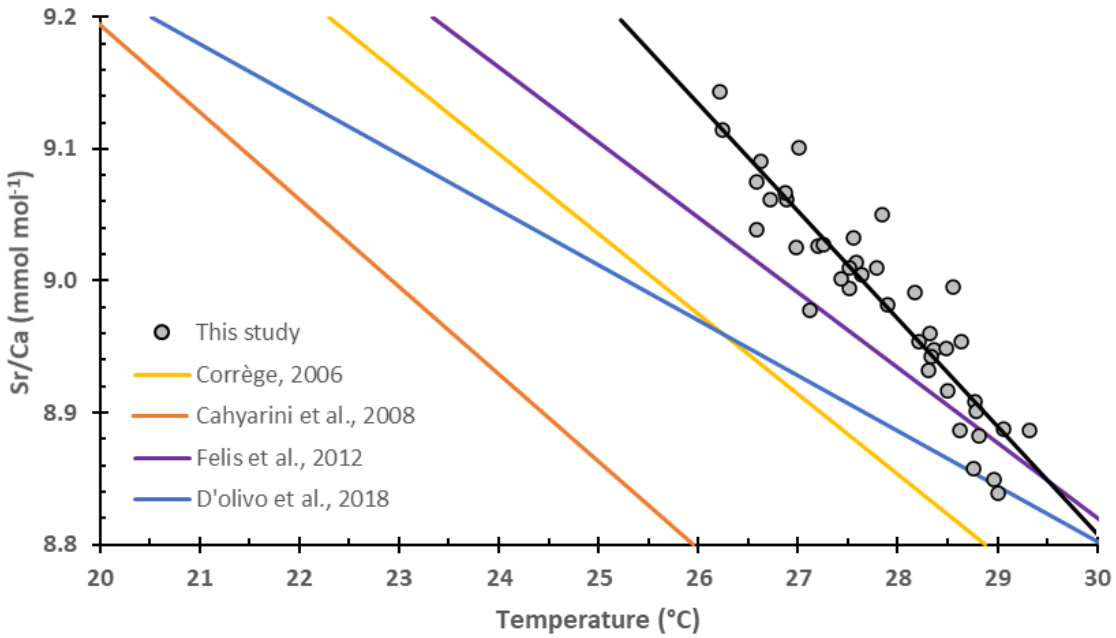

Figure 3 Sr/Ca ratios against temperature for sample MAU-140 of this study, along with the linear regression compared to a representative selection of linear regressions from the literature consisting of D'Olivo et al. (2018) and Corrège (2006) – universal. Cahyarini et al. (2008) and Felis et al., (2012) – local, Tahiti.

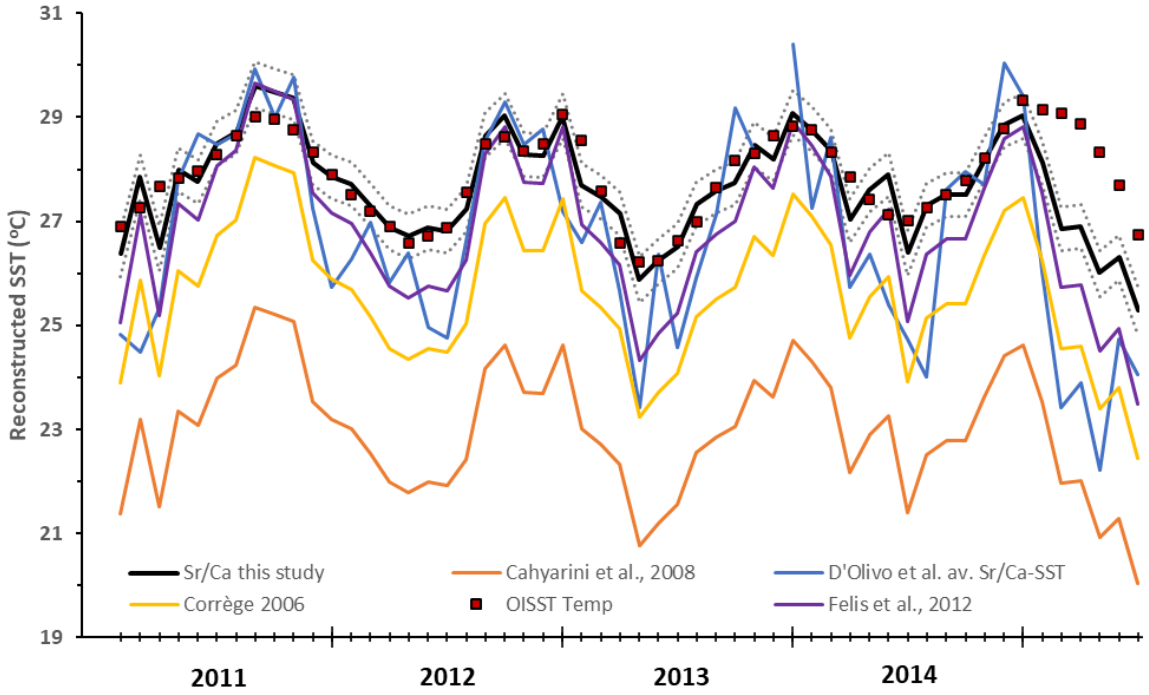

Figure 4 Temperature reconstruction using the different calibration curves and methods proposed in the most relevant literature for Sr/Ca by D'Olivo et al. (2018) and Corrège (2006)-universal. Cahyarini et al. (2008) and Felis et al., (2012) – local Tahiti.

3.4. $\delta^{18}O$

Using the MAU-140 reduced dataset (n = 41) for calibration the fitted regression line of $\delta^{18}O$ on temperature was:

$$\delta^{18}O\ (‰) = -0.166\ (\pm 0.025)\ SST\ (°C) + 0.003\ (\pm 0.689) \quad (3)$$

This produced a SEIP of 0.815 (±0.160) °C.

Our study confirmed within error a slope of – 0.15 ‰/°C that was obtained on a *Porites* microatoll from Christmas Island (McGregor et al., 2011; Woodroffe et al., 2003). The comparison between microatolls and massive *Porites* from the same region indicated very similar slopes with -0.16 (±0.03) ‰/°C from Moorea (Boiseau et al., 1998), – 0.19 (±0.019) ‰/°C from Tahiti (Cahyarini et al., 2008) and -0.168 (±0.012) ‰/°C from Tahiti (Felis et al., 2012) (Figure 5). Each dataset overlapped within error, thus indicating regional reliability of the $\delta^{18}O$ signal. The stability of the external standard analysed in parallel produced a value of -1.70 ‰ and σ = 0.09 (n = 12), providing reasonable confidence in the dataset.

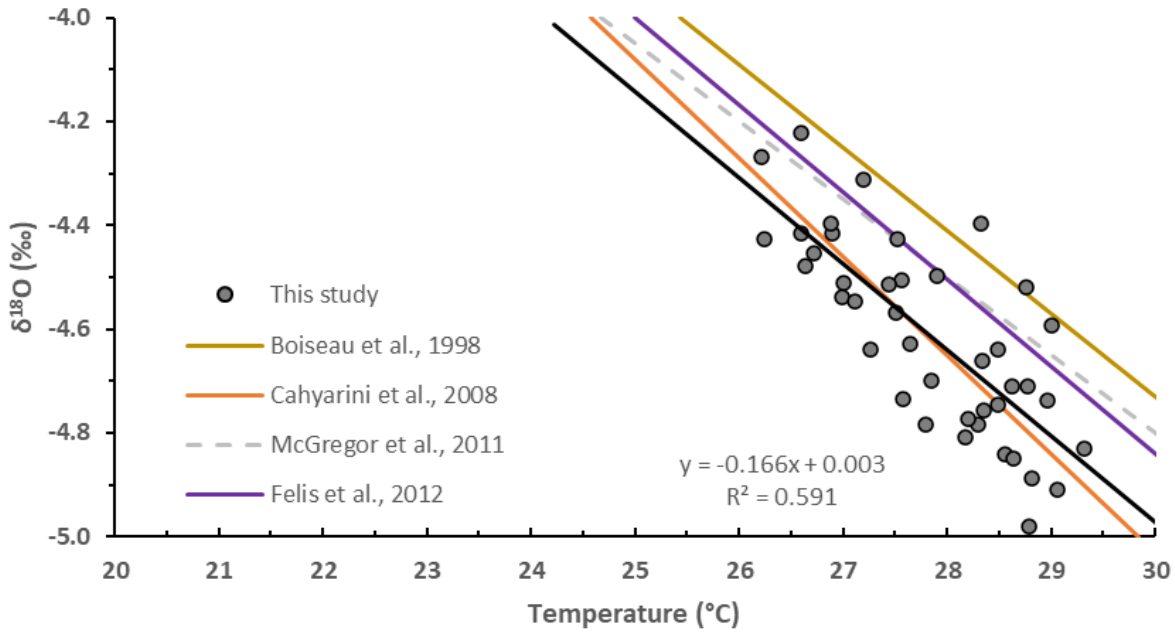

Figure 5 $\delta^{18}O$ values against temperature of sample MAU-140, along with the linear regression compared to linear regressions published in McGregor et al. (2011) – microatoll, Boiseau et al. (1998) – Moorea and Cahyarini et al. (2008) and Felis et al., (2012) - Tahiti.

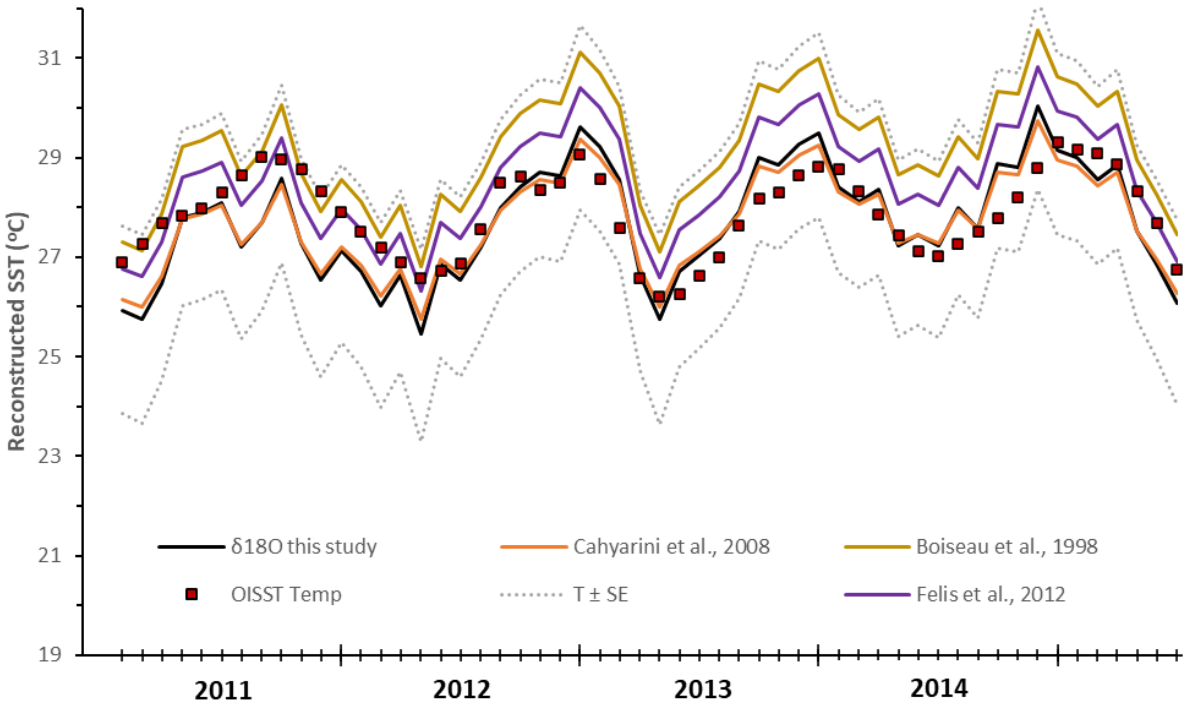

Figure 6 Temperature reconstruction using the formula above for sample MAU-140, along with Optimal Interpolation Sea Surface Temperature (OISST) values. The curve for Maupiti is compared to different $\delta^{18}O$ calibration curves proposed in the representative literature in

McGregor et al. (2011) – microatoll, Boiseau et al. (1998) – Moorea and Cahyarini et al. (2008) and Felis et al., (2012) - Tahiti.

3.5. Li/Mg

The Li/Mg to temperature calibration produced from our microatoll was:

$$\text{Li/Mg (mmol mol}^{-1}\text{)} = -0.073\ (\pm 0.010)\ \text{SST} + 3.495\ (\pm 0.285) \quad (4)$$

The regression model corrected for degrees of freedom produced a SEIP of 0.758 (±0.146) °C.

The methods proposed by Montagna et al. (2014) and D'Olivo et al. (2018) were applied and tested on the MAU-140 microatoll sample. The calibration curve from our sample was compared to that of the two previous studies (Figure 7). The calibration curves were reasonably similar, where the curve of our study displayed the same trend as Montagna et al. (2014) with only a slight offset. The final calibration curve for D'Olivo et al. (2018) followed their method and utilised the average Li/Mg values across the range of calibrations stated in their methodology.

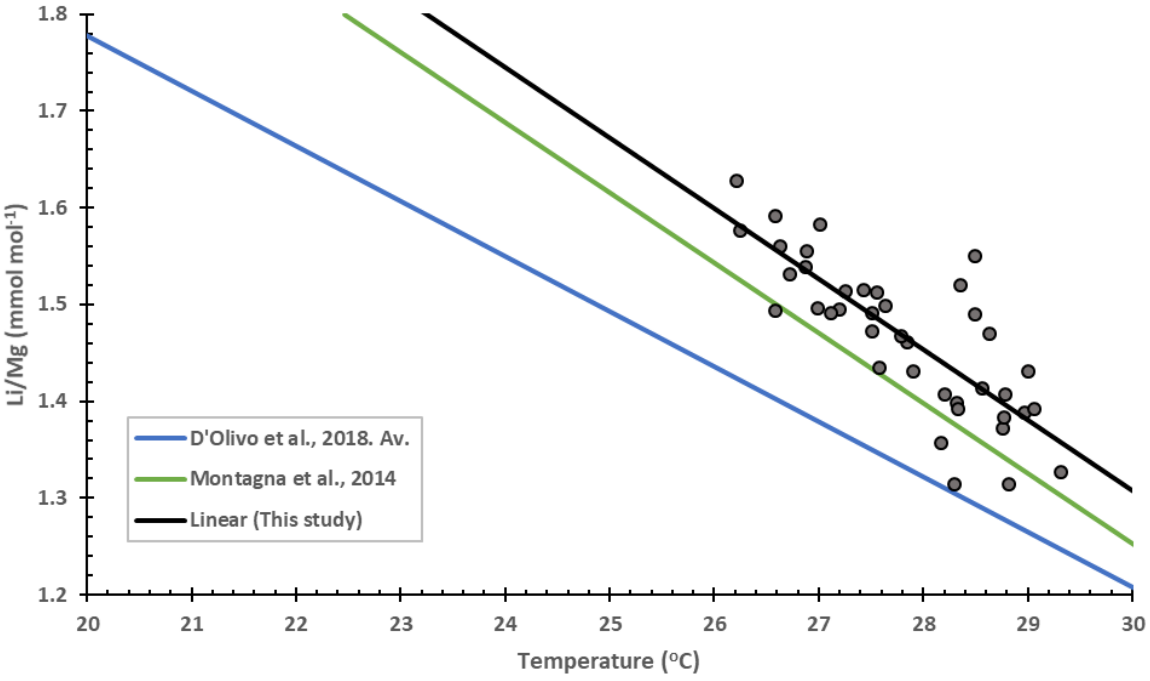

Figure 7 Li/Mg ratios against temperature from this study, along with the linear regression for the sample MAU-140 compared to the regression curves of D'Olivo et al. (2018) and Montagna et al. (2014).

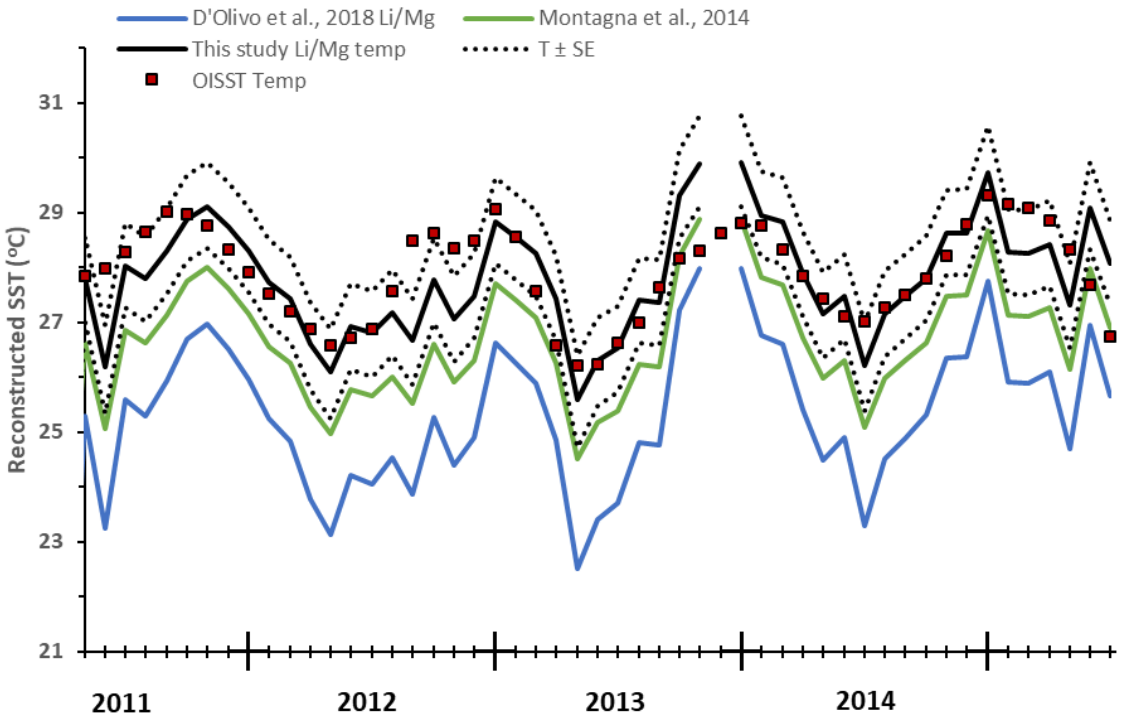

Figure 8 Temperature reconstruction for sample MAU-140 using the Li/Mg data along with Optimal Interpolation Sea Surface Temperature (OISST) values. Data from D'Olivo et al. (2018) and Montagna et al. (2014) were included for comparison.

The Li/Mg curve proposed by D'Olivo et al. (2018) underestimated the actual temperature by about 3°C. The Li/Mg calibration of Montagna et al. (2014) was closer to our calibration, just over one standard error apart in temperature reconstruction. The nature of the Li/Mg data did reconstruct the temperature trends; however, it did not clearly pick out smaller scale features such as the double austral summer peak in 2012. Most of the prediction was within one standard error except for overestimating temperatures during the austral summer of 2013.

As described in section 3.2, the universal calibration from D'Olivo et al. (2018) where Li/Mg was empirically corrected with Sr/Ca produced the best result. However, Zinke et al. (2019) found that, although the universal Li/Mg result worked well, using just the Sr/Ca ratio alone produced a better result. Our results confirmed these findings.

3.6. Sr-U

Here, we applied the method proposed by DeCarlo et al. (2016) using the U/Ca ratio to adjust for potential vital effects in the Sr/Ca signal.

Measured Sr/Ca ratios in the sample MAU-140 ranged from 8.80 to 9.09 mmol mol^{-1} with an average value of 8.93 and SD 0.07 mmol mol^{-1}. U/Ca ratios ranged from 1.08 - 1.29 µmol mol^{-1}, mean 1.20 and SD 0.05 µmol mol^{-1}. These were similar to the values obtained by DeCarlo et

al. (2016) from massive *Porites* corals from four different locations (Red Sea, Western Pacific and two in the Central Pacific) (See Figure 9 where our data were plotted on the same scale and shown alongside Fig. 1a from DeCarlo et al., 2016).

The reverse regression equation from DeCarlo et al. (2016):

$$\mathbf{SST\ (^{o}C) = (-11 \pm 1)\ (Sr\text{-}U - 9) + (28.1 \pm 0.1)} \qquad \mathbf{(5)}$$

with their median value for U/Ca of 1.1 µmol mol^{-1} applied on the reduced dataset of MAU-140 as per the Sr/Ca, $\delta^{18}O$ and Li/Mg methods. The mean temperature was estimated to 29.97 (±0.46)^{o}C. This compared poorly to the actual mean temperature throughout growth as measured from the OISST data of 27.81^{o}C (SD 0.86).

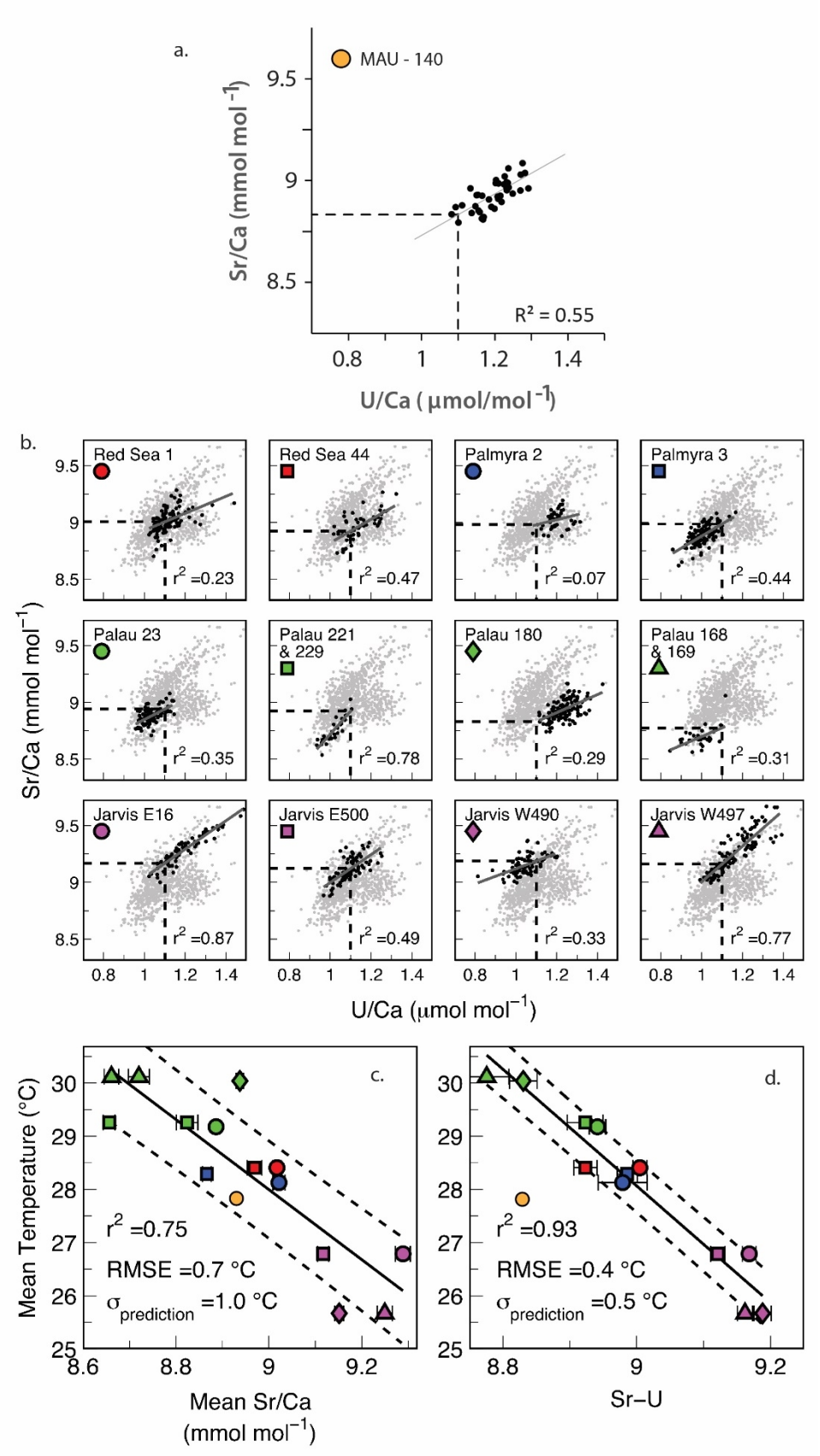

315

316 *Figure 9 Sr-U data of sample MAU-140 from Maupiti. For comparison, data of various sites to*
317 *compare and evaluate the method on a microatoll are reproduced from DeCarlo et al. (2016).*

The mean Sr/Ca value at 8.93 mmol mol^{-1} was similar to the value derived from corals studied in DeCarlo et al. (2016) (see Figure 9b). However, when the U/Ca value of 1.1 µmol mol^{-1} was used to normalise Sr/Ca and calculate the Sr-U value, the resulting temperature prediction overestimated the SST and was outside of the range from DeCarlo et al. (2016), as seen in Figure 9c. This result clearly showed that directly applying that method to our coral data did not improve the temperature estimate. To be applicable to our material, a U/Ca value of 1.29 µmol mol^{-1} would have been required in DeCarlo et al. (2016)'s equation.

We ran a multivariate ANOVA analysis to understand the relationship between Sr/Ca, U/Ca and SST. Fitting a regression model of temperature against Sr/Ca resulted in an R^2 of 0.668. This increased to 0.715 when the U/Ca term was added which was a statistically significant improvement in fit (p-value 0.017). The pattern observed in our data when regressed this way round did indeed confirm that including the U/Ca signal improved the proportion of variance explained (R^2). As discussed in the methods section on the standard versus reverse regression (further detailed in supplementary material S3), the use of the dimensionless R^2 metric will mislead into believing that the prediction is better. However, it is simply showing that the model explains more of the percentage of variability. Using the correct regression of Sr/Ca and U/Ca on temperature, we can estimate temperature by inverse prediction. The inverse prediction is essential when considering the error structure of the regression model and its effect on an estimated temperature. When the inverse prediction was performed on our ICP-MS dataset, the SEIP for the model Sr/Ca against temperature was 0.618 (±0.100) °C. When the U/Ca variable was added to the model, in other words, the regression of Sr/Ca on temperature was adjusted for U/Ca as a covariate, the proportion of variance in the Sr/Ca ratio accounted for (R^2) increased, but the standard error of the inverse prediction increased to 0.808 (±0.153) °C which was not desirable.

3.7. Polynesian microatoll calibrations

Key summary statistics for each of the optimised methods on the MAU-140 sample are presented in

	δ18O	**Li/Mg**	**Sr/Ca adjusted for U/Ca**	**Sr/Ca**
N	41	40	40	41
Slope (±SE)	-0.166 (±0.025) ‰ $°C^{-1}$	-0.073 (±0.010) mmol mol^{-1} $°C^{-1}$	-0.051 (±0.012) mmol mol^{-1} $°C^{-1}$	-0.082 (±0.006) mmol mol^{-1} $°C^{-1}$
Intercept	0.003 (±0.701)	3.495 (±0.280)	9.879 (±0.514)	11.256 (±0.170)

(±SE)	‰	mmol mol^{-1}	mmol mol^{-1}	mmol mol^{-1}
R^2	0.591	0.636	0.715	0.852
RSS	0.56656	0.088709	0.063759	0.034435
RDF	30	30	37	31
MSE	0.0189	0.00296		0.00111
Root MSE	0.1374	0.05438		0.03333
SEIP (±SE) °C	**0.829 (±0.165)**	**0.745 (±0.141)**	**0.809 (±0.153)**	**0.415 (±0.062)**

Table 2. The results showed that $\delta^{18}O$, Li/Mg and Sr/Ca adjusted for U/Ca all showed a similar SEIP value around 0.8 °C, but the Sr/Ca method stood out with a considerably lower SEIP of 0.41 °C. The detailed analysis of all methods optimised for our local sample clearly showed that the Sr/Ca method produced the calibration with the smallest error and best temperature estimate. For Li/Mg signal, we did not apply an empirical combination of Li/Mg and Sr/Ca as per D'Olivo et al. (2018). Instead, we refer to section 3.2 where we applied calibration equations directly from the literature. We explored the consequences of adding U/Ca values to Sr/Ca results to obtain a temperature estimate using the regression with inverse prediction. The R^2 value was high (meaning the variance was largely explained); however, it was misleading as the SEIP in °C was less accurate than the Li/Mg method.

	$\delta^{18}O$	**Li/Mg**	**Sr/Ca adjusted for U/Ca**	**Sr/Ca**
N	41	40	40	41
Slope (±SE)	-0.166 (±0.025) ‰ °C^{-1}	-0.073 (±0.010) mmol mol^{-1} °C^{-1}	-0.051 (±0.012) mmol mol^{-1} °C^{-1}	-0.082 (±0.006) mmol mol^{-1} °C^{-1}
Intercept (±SE)	0.003 (±0.701) ‰	3.495 (±0.280) mmol mol^{-1}	9.879 (±0.514) mmol mol^{-1}	11.256 (±0.170) mmol mol^{-1}
R^2	0.591	0.636	0.715	0.852
RSS	0.56656	0.088709	0.063759	0.034435
RDF	30	30	37	31
MSE	0.0189	0.00296		0.00111

Root MSE	0.1374	0.05438		0.03333
SEIP (±SE) °C	**0.829 (±0.165)**	**0.745 (±0.141)**	**0.809 (±0.153)**	**0.415 (±0.062)**

Table 2 Comparison of $\delta^{18}O$, Li/Mg, Sr/Ca adjusted for U/Ca and Sr/Ca for estimating temperature by inverse prediction.

3.8. Evaluation of stability and reproducibility of Sr/Ca and $\delta^{18}O$

There are concerns about the reliability of the $\delta^{18}O$ and Sr/Ca methods due to localised offsets and vital effects which may affect individual corals differentially (Corrège, 2006; de Villiers et al., 1995). To counteract this deficiency, slopes and intercepts from multiple corals from the same area can be averaged together to create a regional calibration smoothing out the offsets (Felis et al., 2003; Sayani et al., 2019). However, when analysing a single fossil sample, it becomes impossible to identify its specific offset.

To test the robustness and reproducibility of both $\delta^{18}O$ and Sr/Ca, additional modern samples from the same region were assessed, particularly coral samples BOB-478 and BOB-108 from the North and South of Bora-Bora, respectively (Figure 1).

3.8.1. BOB-108

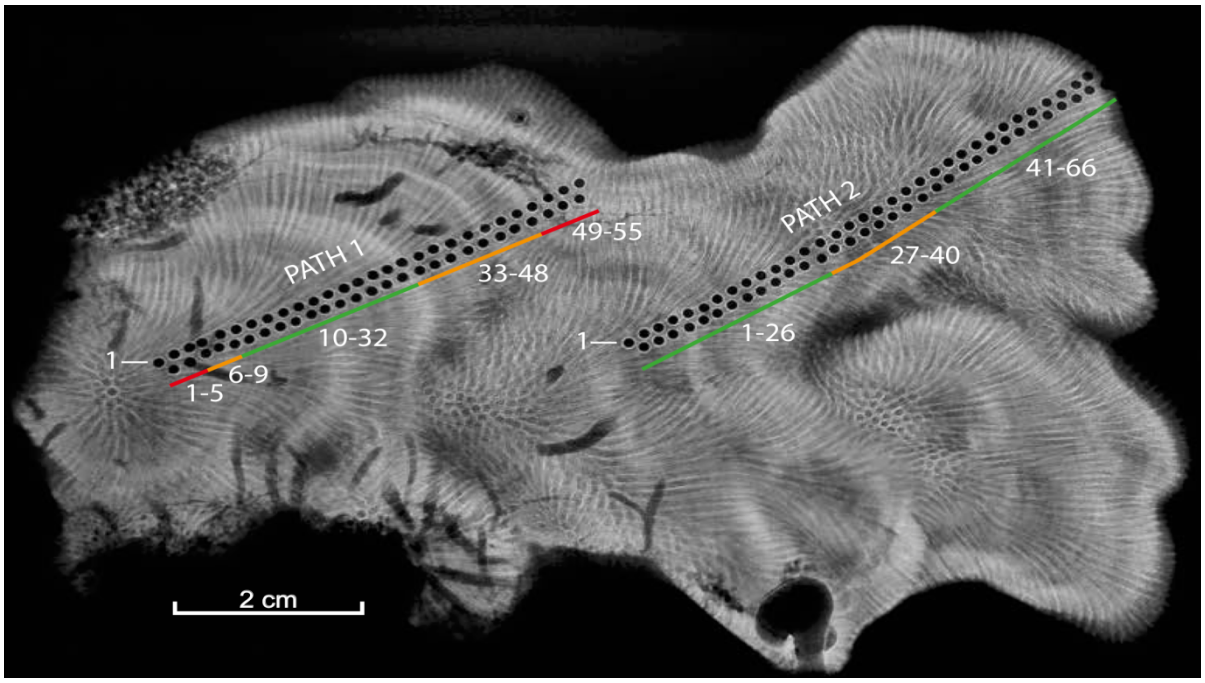

Figure 10 X-radiograph image of the BOB-108 sample. The coloured lines show where the sample points were included in the analysis (green) as they are in line with the corallite growth, where it is doubtful (orange) and red where sample points were excluded.

BOB-108 exhibited a more complex growth in multiple directions (Figure 10). Slabbing was done along the dominant growth axis, but a single continuous sampling track was impossible to identify. The SEM images revealed a generally good preservation in the main part of the coral skeleton. There were issues of pore infilling visible near the upper surface of the coral, a region with secondary Mg-rich crystal growth (brucite) related to algal growth (See SEM images, preservation and discussion on brucite crystal in supplementary material S6). This part was discarded from the data analyses below.

Figure 10 shows that many samples were taken in areas where the growth axis was no longer parallel to the slab cut axis. Those samples were excluded from the interpretation as they likely would produce unreliable results (e.g. DeLong et al., 2013). Combining the two transect lines would have been possible through estimation following barely visible annual density growth bands (Figure 10) but could have brought significant uncertainties. The sample was therefore reduced to 28 data points, thus covering two years of strongly reliable data.

After analysis, it was reconfirmed that applying the hinge points on peaks and troughs produced the best model for the temperature interpolation, explaining most of variations without becoming overfitted.

3.8.2. BOB-478

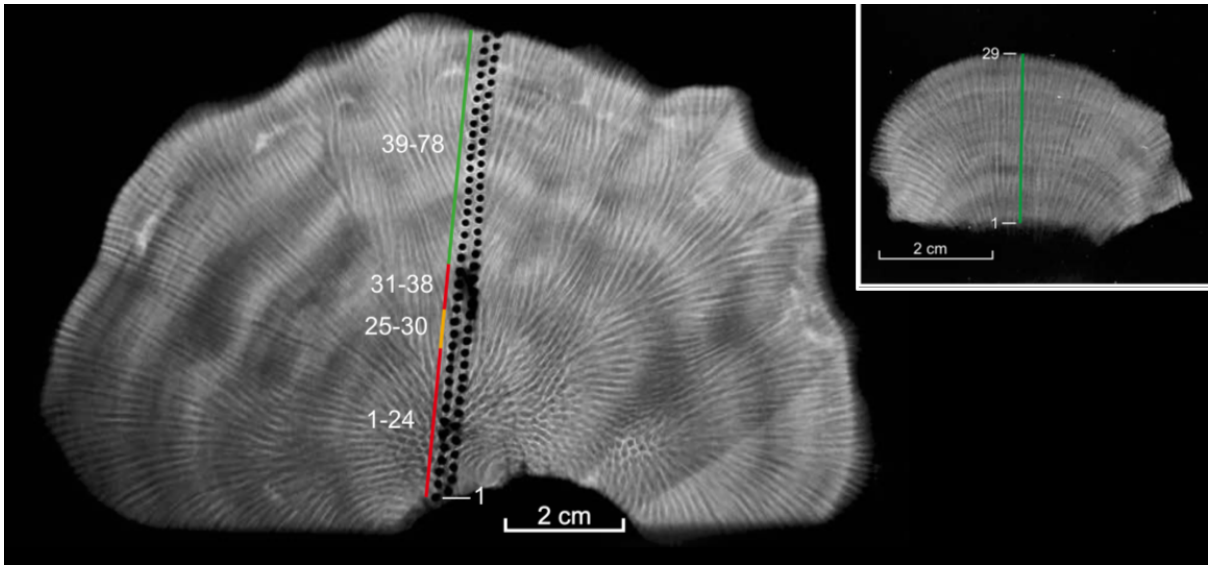

Figure 11 X-radiographs of BOB-48 and BOB-47. They are combined to produce dataset BOB-478 (see text). The green line is alongside the samples that the X-ray shows where sampling was suitably aligned with corallite growth. The red and orange in this case is where samples were not included in the analysis because of the corallite growth direction.

BOB-47 was an overgrowth adjacent to BOB-48, implying that the data could be combined as the growth occurred over the same time periods. No secondary diagenetic alteration was identified under the SEM (see supplementary material S7). From the sample BOB-48 the first 38 drilled spots were not parallel to the growth axis and were excluded from data analysis

(Figure 11). The data from BOB-47 and BOB-48 were combined by averaging contemporaneous samples to create the dataset BOB-478, i.e. the most suitable hinge point and interpolation model was the one of peaks and troughs.

3.8.3. Reproducibility of Sr/Ca

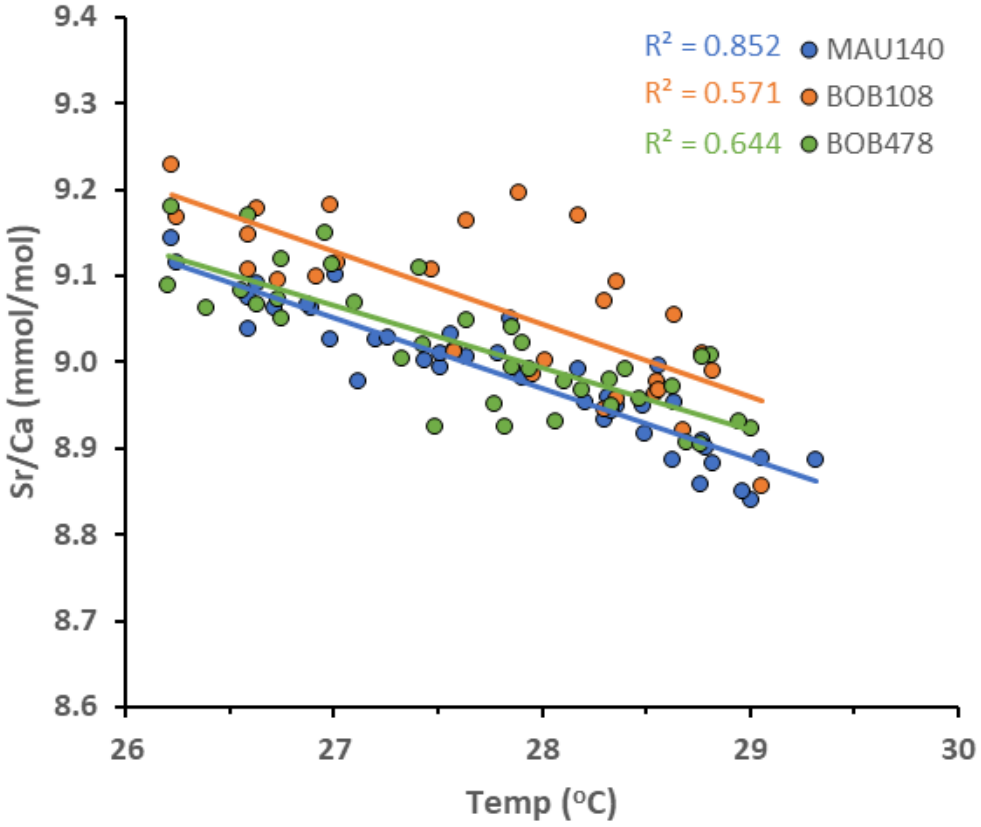

Figure 12 Sr/Ca to temperature relationship of the samples MAU-140, BOB-108 and BOB-478.

Possible offsets of Sr/Ca ratios between corals driven by vital effects were evaluated. The linear regression fits of Sr/Ca on SST for all three corals are shown in Table 3 and Fig. 12. Coral MAU-140 resulted in a SEIP of 0.415 (±0.062)°C; the coral BOB-108 resulted in a SEIP of 0.840 (±0.200)°C and BOB-478 a SEIP of 0.724 (±0.143)°C (Table 3). Importantly, despite the residual errors becoming larger on the two Bora Bora corals as the sample quality deteriorated, the fundamental relationship (slope and intercept) of the Sr/Ca to temperature remained very robust. There was no significant difference between the slopes or intercepts across the corals.

	MAU-140	BOB-108	BOB-478	Combined 3 corals
N	41	28	37	106

Sr/Ca				
Mean	8.9842	9.0627	9.0178	9.0166
SD	0.0763	0.0975	0.0757	0.0872
Temperature (°C)				
Mean	27.8321	27.7713	27.6716	27.7600
SD	0.8633	0.8747	0.8427	0.8538
Regression				
Hinges	9	4	8	21
Intercept (±SE)	11.256 (±0.173)	11.402 (±0.432)	11.012 (±0.286)	11.229 (±0.195)
Slope (±SE)	-0.082 (±0.006)	-0.084 (±0.016)	-0.072 (±0.010)	-0.080 (±0.007)
R^2	0.852	0.571	0.644	0.609
RSS	0.0344	0.1101	0.0735	0.3124
RDF	30	23	27	83
MSE	0.0011	0.0048	0.0027	0.0038
Root MSE	0.0339	0.0692	0.0522	0.0613
SEIP (±SE) °C	**0.415 (±0.062)**	**0.840 (±0.200)**	**0.724 (±0.143)**	**0.770 (±0.090)**

Table 3 Sr/Ca to temperature model analysis, for each coral (MAU-140, BOB-108 and BOB-478) and combined calibrations to Optimum Interpolation Sea Surface Temperature (OISST).

3.8.4. Reproducibility of $\delta^{18}O$

$\delta^{18}O$ is affected by a combination of temperature and salinity (controlled in the present case by precipitation intensity). Data were collected on the four corals and combined into three coral records (same sampling points as for Sr/Ca). It was possible to observe an occasional lag in the $\delta^{18}O$ curve compared to the Sr/Ca curve but adjusting the tie points for the temperature interpolation to optimise for $\delta^{18}O$ did not significantly improved model fit (supplementary material S4).

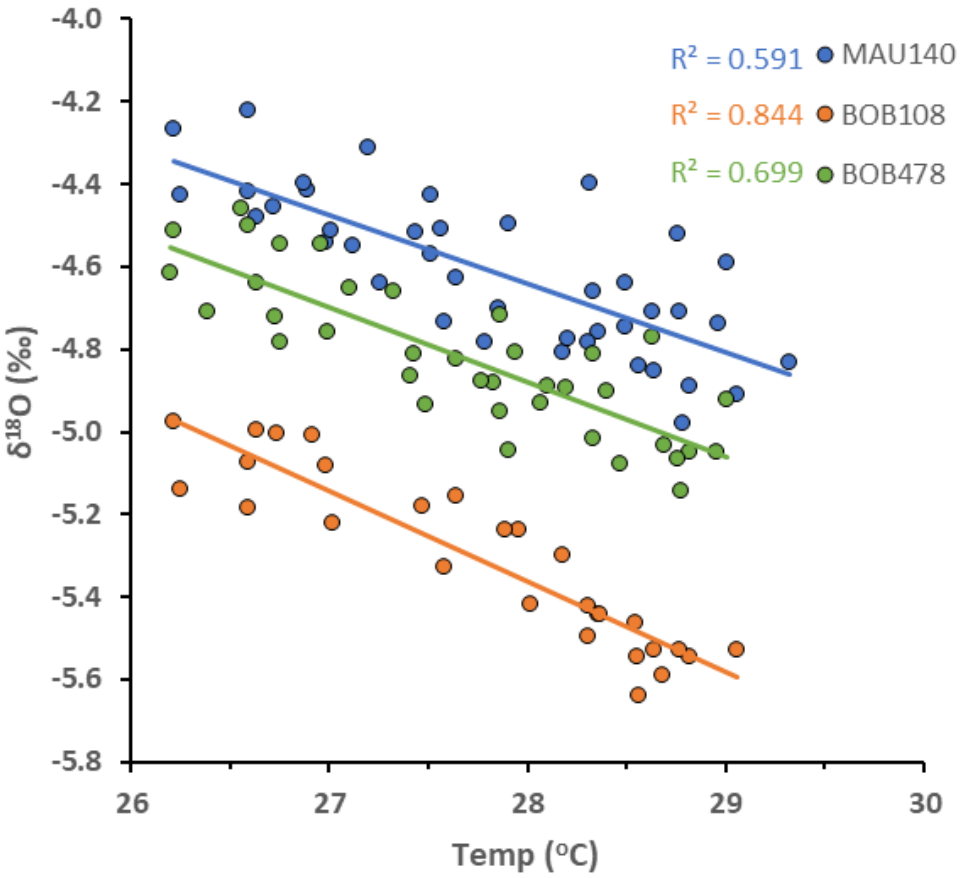

Figure 13 $\delta^{18}O$ values against temperature for sample MAU-140 in blue, BOB-478 in orange and BOB-108 in green, along with the respective regression curves.

Linear regression fits of $\delta^{18}O$ against SST for each coral are presented separately and a combined regression model (Table 4). The SEIP derived from sample MAU-140 was 0.829 (±0.165) °C, as seen previously in Table 2. Data obtained on the BOB-108 sample revealed the smallest SEIP but relied on a reduced dataset (N = 28) with only sample points validated from the X-ray imagery (see above). There was a significant difference between calibration curves produced by each of the three coral samples (Figure and Table). When combining the three corals into a single calibration model, purely statistically speaking, the quality of fit (residual mean square) was very similar for a model fitting a single slope but three different intercepts or a model fitting a single intercept but three different slopes. Considering the two, the model with a single common slope and three different intercepts, one for each coral, was more realistic and relevant. The variation (in intercept or can be read individual offset) across the three corals meant that the SEIP became considerably greater when combined into a single calibration (Table).

	MAU-140	BOB-108	BOB-478	Combined 3 corals
N	41	28	37	106

$\delta^{18}O$				
Mean	-4.6129	-5.3107	-4.8207	-4.8698
St Dev	0.1862	0.2080	0.1822	0.3379
Temperature (°C)				
Mean	27.8321	27.7713	27.6716	27.7600
St Dev	0.8633	0.8747	0.8427	0.8538
Regression				
Hinges	9	4	8	21
Intercept (±SE) ‰	0.003 (±0.701)	0.756 (±0.544)	0.183 (±0.632)	0.070 (±1.078)
Slope (±SE) ‰ $°C^{-1}$	-0.166 (±0.025)	-0.218 (±0.020)	-0.181 (±0.023)	-0.178 (±0.039)
R^2	0.5914	0.8440	0.6992	0.2022
RSS	0.566562	0.182196	0.359586	9.565307
RDF	30	23	27	83
MSE	0.0189	0.0079	0.0133	0.1152
Root MSE	0.1374	0.0890	0.1154	0.3395
SEIP (±SE) °C	**0.829 (±0.165)**	**0.407 (±0.070)**	**0.638 (±0.118)**	**1.908 (±0.442)**

Table 4 Summary of data used in statistics for the regression of $\delta^{18}O$ to temperature for each coral and for a model where all three are combined.

4. Conclusion

This study demonstrates that Sr/Ca in *Porites* microatolls is a precise and reliable proxy for reconstructing sea-surface temperatures, with a standard error of the inverse prediction of 0.415 (±0.062) °C. The Sr/Ca to temperature relationship remained very consistent across multiple corals independent of sample quality. The precision and reliability across multiple corals were remarkable and merit to be repeated on microatolls growing in similar environmental conditions from other regions. The nature of microatolls continually growing

at the same water depth most likely plays a role in the consistency and reproducibility of the signal. The local calibration that we obtained in French Polynesia can be used as a reliable calibration for the tropical Pacific, and the reconstruction of Holocene sea-surface temperatures based on *Porites* microatolls.

$\delta^{18}O$ resulted in a reasonable confidence for the reconstructed relative temperature range (seasonality), but outliers and significant local offsets meant large errors in absolute temperature predictions. The $\delta^{18}O$-SST relationship was similar to that of previously studied French Polynesian massive *Porites.* The local offset between our samples needs further investigation to explain whether a single universal calibration can be applied to microatolls. Replication in other locations will be necessary to gain further insight into this proxy.

Assessing the key coral paleothermometry techniques established in the literature, we found, where no local calibration is available, the Li/Mg ratio empirically corrected for Sr/Ca was the method that best balanced bias and precision. The Sr-U method did not produce an accurate result on our microatoll sample despite the Sr/Ca and U/Ca values being within the expected range. Exploring in detail showed that the method itself with the regression model used was the most likely source of error.

Our study shows that *Porites* microatolls accurately and reliably record sea-surface temperatures. Our regional calibration (Sr/Ca = -0.082 ± 0.006 SST + 11.256 ± 0.170) for the French Polynesian islands in the Tropical South Pacific applies to sea surface, the targeted proxy for paleoclimate reconstruction. This is a fundamental and significant step towards reconstructing sea-surface temperature because *Porites* microatolls grow close to the sea-air interface, whereas dome-shaped *Porites* corals grow in a wide range between near surface and roughly 20 m water depth.

Acknowledgements

Field campaigns and sampling were conducted in the frame of the HOLOREEFS project. The support of the Department of Earth Sciences, University of Geneva, is acknowledged. The support of Serge Planes and his team at CRIOBE in Moorea, French Polynesia, is thankfully acknowledged. The study benefited from funding through the Swiss National Science Foundation (Project 133771).

Data availability

Data for this submission is attached as supplementary. The temperature data obtained for this study is the AVHRR OISST v2 dataset (Banzon et al., 2016; Reynolds et al., 2007). The data is available at doi:10.7289/V5SQ8XB5 or through https://www.ncdc.noaa.gov/oisst. For figures featuring in the Appendix, we also used MétéoFrance station data which is accessible directly from them upon request through https://donneespubliques.meteofrance.fr.

References

Alibert, C., & McCulloch, M. T. (1997). Strontium/calcium ratios in modern porites corals From the Great Barrier Reef as a proxy for sea surface temperature: Calibration of the thermometer and monitoring of ENSO. *Paleoceanography, 12*(3), 345-363. doi:10.1029/97pa00318

Alpert, A. E., Cohen, A. L., Oppo, D. W., DeCarlo, T. M., Gaetani, G. A., Hernandez-Delgado, E. A., et al. (2017). Twentieth century warming of the tropical Atlantic captured by Sr-U paleothermometry. *Paleoceanography, 32*(2), 146-160. doi:10.1002/2016pa002976

Antonioli, G. (2018). Assessment of sea-surface temperature using modern coral microatolls from Society Islands, French Polynesia. MSc Thesis University of Geneva, Switzerland, 92pp.

Banzon, V., Smith, T. M., Chin, T. M., Liu, C. Y., & Hankins, W. (2016). A long-term record of blended satellite and in situ sea-surface temperature for climate monitoring, modeling and environmental studies. *Earth System Science Data, 8(1), 165-176.* doi:dx.doi.org/10.5194/essd-8-165-2016

Boiseau, M., Juillet-Leclerc, A., Yiou, P., Salvat, B., Isdale, P., & Guillaume, M. (1998). Atmospheric and oceanic evidences of El Niño-Southern Oscillation events in the south central Pacific Ocean from coral stable isotopic records over the last 137 years. *Paleoceanography, 13*(6), 671-685. doi:10.1029/98pa02502

Cahyarini, S. Y., Pfeiffer, M., Timm, O., Dullo, W.-C., & GarbeSchönberg, D. (2008). Reconstructing seawater δ18O from paired coral δ18O and Sr/Ca ratios: Methods, error analysis and problems, with examples from Tahiti (French Polynesia) and Timor (Indonesia). *Geochimica et Cosmochimica Acta, 72*(12), 2841-2853. doi:doi.org/10.1016/j.gca.2008.04.005

Cantarero, S., Tanzil, J., & Goodkin, N. (2017). Simultaneous analysis of Ba and Sr to Ca ratios in scleractinian corals by inductively coupled plasma optical emissions spectrometry. *Limnology and Oceanography: Methods, 15*(1), 116-123. doi:10.1002/lom3.10152

Cashin, P., Mohaddes, K., & Raissi, M. (2017). Fair weather or foul? The macroeconomic effects of El Nino. *Journal of International Economics, 106*, 37-54. doi:10.1016/j.jinteco.2017.01.010

Chen, X., Wei, G., Deng, W., Liu, Y., Sun, Y., Zeng, T., & Xie, L. (2015). Decadal variations in trace metal concentrations on a coral reef: Evidence from a 159 year record of Mn, Cu, and V in a Porites coral from the northern South China Sea. *Journal of Geophysical Research: Oceans, 120*(1), 405-416. doi:10.1002/2014jc010390

Corrège, T. (2006). Sea surface temperature and salinity reconstruction from coral geochemical tracers. *Palaeogeography, Palaeoclimatology, Palaeoecology, 232*(2-4), 408-428. doi:10.1016/j.palaeo.2005.10.014

D'Olivo, J. P., Sinclair, D. J., Rankenburg, K., & McCulloch, M. T. (2018). A universal multi-trace element calibration for reconstructing sea surface temperatures from long-lived Porites corals: Removing 'vital-effects'. *Geochimica et Cosmochimica Acta, 239*, 109-135. doi:doi.org/10.1016/j.gca.2018.07.035

de Villiers, S., Nelson, B. K., & Chivas, A. R. (1995). Biological controls on coral Sr/Ca and δ18O reconstructions of sea surface temperatures. *Science, 269*(5228), 1247-1249. doi:10.1126/science.269.5228.1247

de Villiers, S., Shen, G. T., & Nelson, B. K. (1994). The SrCa-temperature relationship in coralline aragonite: Influence of variability in (SrCa)seawater and skeletal growth parameters. *Geochimica et Cosmochimica Acta, 58*(1), 197-208. doi:doi.org/10.1016/0016-7037(94)90457-X

DeCarlo, T. M., Gaetani, G. A., Cohen, A. L., Foster, G. L., Alpert, A. E., & Stewart, J. A. (2016). Coral Sr-U thermometry. *Paleoceanography, 31*(6), 626-638. doi:doi:10.1002/2015PA002908

Delesalle, B., Galzin, R., and Salvat, B. . (1985). "French polynesian coral reefs" *Proceedings of the 5th International Coral Reef Congress, Papeete, Vol. 1,* (Tahiti: IABO), 1–554.

538 DeLong, K. L., Quinn, T. M., Taylor, F. W., Shen, C.-C., & Lin, K. (2013). Improving coral-base
539 paleoclimate reconstructions by replicating 350years of coral Sr/Ca variations.
540 *Palaeogeography, Palaeoclimatology, Palaeoecology, 373*, 6-24.
541 doi:doi.org/10.1016/j.palaeo.2012.08.019
542 Demidenko, E., Williams, B. B., Flood, A. B., & Swartz, H. M. (2013). Standard error of inverse prediction
543 for dose–response relationship: approximate and exact statistical inference. *Statistics in*
544 *Medicine, 32*(12), 2048-2061. doi:10.1002/sim.5668
545 Draper, N. R., & Smith, H. (1981). *Applied Regression Analysis.* (Second edition ed.): John Wiley &
546 Sons
547 Felis, T., Merkel, U., Asami, R., Deschamps, P., Hathorne, E. C., Kölling, M., et al. (2012). Pronounced
548 interannual variability in tropical South Pacific temperatures during Heinrich Stadial 1. *Nature*
549 *Communications, 3*(1), 965. doi:10.1038/ncomms1973
550 Felis, T., Pätzold, J., & Loya, Y. (2003). Mean oxygen-isotope signatures in Porites spp. corals: inter-
551 colony variability and correction for extension-rate effects. *Coral Reefs, 22*(4), 328-336.
552 doi:10.1007/s00338-003-0324-3
553 Gaetani, G. A., & Cohen, A. L. (2006). Element partitioning during precipitation of aragonite from
554 seawater: A framework for understanding paleoproxies. *Geochimica et Cosmochimica Acta,*
555 *70*(18), 4617-4634. doi:doi.org/10.1016/j.gca.2006.07.008
556 Gaetani, G. A., Cohen, A. L., Wang, Z., & Crusius, J. (2011). Rayleigh-based, multi-element coral
557 thermometry: A biomineralization approach to developing climate proxies. *Geochimica et*
558 *Cosmochimica Acta, 75*(7), 1920-1932. doi:doi.org/10.1016/j.gca.2011.01.010
559 Grove, C. A., Rodriguez-Ramirez, A., Merschel, G., Tjallingii, R., Zinke, J., Macia, A., & Brummer, G.-J.
560 A. (2015). UV-spectral luminescence scanning: technical updates and calibration
561 developments. In I. W. Croudace & R. G. Rothwell (Eds.), *Micro-XRF Studies of Sediment Cores:*
562 *Applications of a non-destructive tool for the environmental sciences* (pp. 563-581). Dordrecht:
563 Springer Netherlands.
564 Hallmann, N., Camoin, G., Eisenhauer, A., Botella, A., Milne, G. A., Vella, C., et al. (2018). Ice volume
565 and climate changes from a 6000 year sea-level record in French Polynesia. *Nature*
566 *Communications, 9*(1), 285. doi:10.1038/s41467-017-02695-7
567 Hallmann, N., Camoin, G., Eisenhauer, A., Samankassou, E., Vella, C., Botella, A., Milne G.A., Pothin,
568 V., Dussouillez, P., Fleury, J., Fietzke, J. & Goepfert, T. (*in press*). Reef response to sea-level and
569 environmental changes in the Central South Pacific over the past 6000 years. *Global and*
570 *Planetary Change*. doi.org/10.1016/j.gloplacha.2020.103357.
571 Hathorne, E. C., Felis, T., Suzuki, A., Kawahata, H., & Cabioch, G. (2013). Lithium in the aragonite
572 skeletons of massive Porites corals: A new tool to reconstruct tropical sea surface
573 temperatures. *Paleoceanography, 28*(1), 143-152. doi:10.1029/2012pa002311
574 Hathorne, E. C., Gagnon, A., Felis, T., Adkins, J., Asami, R., Boer, W., et al. (2013). Interlaboratory study
575 for coral Sr/Ca and other element/Ca ratio measurements. Geochemistry, Geophysics,
576 Geosystems, 14(9), 3730-3750. doi:10.1002/ggge.20230
577 Inoue, M., Ishikawa, D., Miyaji, T., Yamazaki, A., Suzuki, A., Yamano, H., et al. (2014). Evaluation of Mn
578 and Fe in coral skeletons (Porites spp.) as proxies for sediment loading and reconstruction of
579 50 yrs of land use on Ishigaki Island, Japan. *Coral Reefs, 33*(2), 363-373. doi:10.1007/s00338-
580 014-1128-3
581 Krause, S., Liebetrau, V., Nehrke, G., Damm, T., Büsse, S., Leipe, T., et al. (2019). Endolithic algae affect
582 modern coral carbonate morphology and chemistry. Frontiers in Earth Science, 7(304).
583 doi:10.3389/feart.2019.00304
584 Marriott, C. S., Henderson, G. M., Belshaw, N. S., & Tudhope, A. W. (2004). Temperature dependence
585 of δ7Li, δ44Ca and Li/Ca during growth of calcium carbonate. *Earth and Planetary Science*
586 *Letters, 222*(2), 615-624. doi:doi.org/10.1016/j.epsl.2004.02.031

McGregor, H. V., Fischer, M. J., Gagan, M. K., Fink, D., & Woodroffe, C. D. (2011). Environmental control of the oxygen isotope composition of Porites coral microatolls. *Geochimica et Cosmochimica Acta, 75*(14), 3930-3944. doi:doi.org/10.1016/j.gca.2011.04.017

McLean, R. F., Stoddart, D. R., Hopley, D., & Polach, H. (1978). Sea Level Change in the Holocene on the Northern Great Barrier Reef. Philosophical Transactions of the Royal Society of London. Series A, Mathematical and Physical Sciences, 291(1378), 167-186.

Meibom, A., Mostefaoui, S., Cuif, J.-P., Dauphin, Y., Houlbreque, F., Dunbar, R., & Constantz, B. (2007). Biological forcing controls the chemistry of reef-building coral skeleton. *Geophysical Research Letters, 34*(2). doi:10.1029/2006gl028657

Meltzner, A. J. & Woodroffe, C. D. (2015). Coral microatolls. In I. Shennan, A. J. Long & B. P. Horton (Eds.), Handbook of Sea-Level Research (pp. 125-145). United Kingdom: John Wiley & Sons.

Montagna, P., McCulloch, M., Douville, E., López Correa, M., Trotter, J., Rodolfo-Metalpa, R., et al. (2014). Li/Mg systematics in scleractinian corals: Calibration of the thermometer. *Geochimica et Cosmochimica Acta, 132*, 288-310. doi:doi.org/10.1016/j.gca.2014.02.005

Neter, J., Wasserman, W., & Kutner, M. H. (1985). *Applied Linear Statistical Models: Regression, Analysis of Variance, and Experimental Designs.* Homewood, IL: Richard D. Irwin.

Okai, T., Suzuki, A., Kawahata, H., Terashima, S., & Imai, N. (2002). Preparation of a New Geological Survey of Japan Geochemical Reference Material: Coral JCp-1. *Geostandards Newsletter, 26*(1), 95-99. doi:10.1111/j.1751-908X.2002.tb00627.x

Parker, D. E., Basnett, T. A., Brown, S. J., Gordon, M., Horton, E. B., & Rayner, N. A. (2000). Climate Observations - The Instrumental Record. Space Science Reviews, 94(1), 309-320. doi:10.1023/A:1026787727530Reynolds, R. W., Smith, T. M., Liu, C., Chelton, D. B., Casey, K. S., & Schlax, M. G. (2007). Daily high-resolution-blended analyses for sea surface temperature. *Journal of Climate, 20*(22), 5473-5496. doi:10.1175/2007jcli1824.1

Rashid, R., Eisenhauer, A., Liebetrau, V., Fietzke, J., Böhm, F., Wall, M., et al. (2020). Early Diagenetic Imprint on Temperature Proxies in Holocene Corals: A Case Study From French Polynesia. *Frontiers in Earth Science, 8*(301). doi:10.3389/feart.2020.00301

Roche, R. C., Perry, C. T., Smithers, S. G., Leng, M. J., Grove, C. A., Sloane, H. J., & Unsworth, C. E. (2014). Mid-Holocene sea surface conditions and riverine influence on the inshore Great Barrier Reef. *The Holocene, 24*(8), 885-897. doi:10.1177/0959683614534739

Ross, C. L., DeCarlo, T. M., & McCulloch, M. T. (2019). Calibration of Sr/Ca, Li/Mg and Sr-U paleothermometry in branching and foliose corals. *Paleoceanography and Paleoclimatology, 34*(8), 1271-1291. doi:10.1029/2018pa003426

Sayani, H., Cobb, K., Cohen, A., Elliott, W., Nurhati, I., Dunbar, R., et al. (2011). Effects of diagenesis on paleoclimate reconstructions from modern and young fossil corals. *Geochimica et Cosmochimica Acta, 75*(21), 6361-6373. doi:10.1016/j.gca.2011.08.026

Sayani, H. R., Cobb, K. M., DeLong, K., Hitt, N. T., & Druffel, E. R. M. (2019). Intercolony δ18O and Sr/Ca variability among Porites spp. corals at Palmyra Atoll: Toward more robust coral-based estimates of climate. *Geochemistry, Geophysics, Geosystems, 20*(11), 5270-5284. doi:10.1029/2019gc008420

Schofield, H. J. (2011). *Holocene changes in mean sea-surface temperatures from Central Pacific fossil microatolls.* (Bachelor of Science (Honours)). University of Wollongong.

Seard, C., Camoin, G., Yokoyama, Y., Matsuzaki, H., Durand, N., Bard, E., et al. (2011). Microbialite development patterns in the last deglacial reefs from Tahiti (French Polynesia; IODP Expedition #310): Implications on reef framework architecture. *Marine Geology, 279*(1), 63-86. doi:https://doi.org/10.1016/j.margeo.2010.10.013

Sinclair, D. J. (2015). RBME coral temperature reconstruction: An evaluation, modifications, and recommendations. *Geochimica et Cosmochimica Acta, 154*, 66-80. doi:10.1016/j.gca.2015.01.006

636 Smith, J. A., Andersen, T. J., Shortt, M., Gaffney, A. M., Truffer, M., Stanton, T. P., et al. (2016). Sub-
637 ice-shelf sediments record history of twentieth-century retreat of Pine Island Glacier. *Nature,*
638 *541*, 77. doi:10.1038/nature20136
639 Smith, S. V., Buddemeier, R. W., Redalje, R. C., & Houck, J. E. (1979). Strontium-calcium thermometry
640 in coral skeletons. *Science, 204*(4391), 404-407. doi:10.1126/science.204.4391.404
641 Smithers, S. G., & Woodroffe, C. D. (2001). Coral microatolls and 20th century sea level in the eastern
642 Indian Ocean. *Earth and Planetary Science Letters, 191*(1), 173-184.
643 doi:doi.org/10.1016/S0012-821X(01)00417-4
644 Spötl, C., & Vennemann, T. W. (2003). Continuous-flow isotope ratio mass spectrometric analysis of
645 carbonate minerals. Rapid Communications in Mass Spectrometry, 17(9), 1004-1006.
646 doi:10.1002/rcm.1010
647 Stoddart, D. R. (1969). Ecology And Morphology of Recent Coral Reefs. Biological Reviews, 44(4), 433-
648 498. doi:10.1111/j.1469-185X.1969.tb00609.x
649 Thompson, D. M., Cole, J. E., Shen, G. T., Tudhope, A. W., & Meehl, G. A. (2014). Early twentieth-
650 century warming linked to tropical Pacific wind strength. *Nature Geoscience, 8*, 117.
651 doi:10.1038/ngeo2321
652 Woodroffe, C., & McLean, R. (1990). Microatolls and recent sea level change on coral atolls. *Nature,*
653 *344*(6266), 531-534. doi:10.1038/344531a0
654 Woodroffe, C. D., Beech, M. R., & Gagan, M. K. (2003). Mid-late Holocene El Niño variability in the
655 equatorial Pacific from coral microatolls. *Geophysical Research Letters, 30*(7).
656 doi:10.1029/2002gl015868
657 Yamano, H., & Watanabe, T. (2016). Coupling Remote Sensing and Coral Annual Band Data to
658 Investigate the History of Catchment Land Use and Coral Reef Status. In H. Kayanne (Ed.), *Coral*
659 *Reef Science: Strategy for Ecosystem Symbiosis and Coexistence with Humans under Multiple*
660 *Stresses* (pp. 47-53). Tokyo: Springer Japan.
661 Yu, K.-F., Zhao, J.-X., Done, T., & Chen, T.-G. (2009). Microatoll record for large century-scale sea-level
662 fluctuations in the mid-Holocene. *Quaternary Research, 71*(3), 354-360.
663 doi:doi.org/10.1016/j.yqres.2009.02.003
664 Zinke, J., D'Olivo, J. P., Gey, C. J., McCulloch, M. T., Bruggemann, J. H., Lough, J. M., & Guillaume, M.
665 M. M. (2019). Multi-trace-element sea surface temperature coral reconstruction for the
666 southern Mozambique Channel reveals teleconnections with the tropical Atlantic.
667 *Biogeosciences, 16*(3), 695-712. doi:10.5194/bg-16-695-2019